J. Membrane Biol. 19, 141–162 (1974)
© by Springer-Verlag New York Inc. 1974

Ionophoric Material Derived From Eel Membrane Preparations

II. Electrical Characteristics

Robert Blumenthal and Adil E. Shamoo

Laboratory of Theoretical Biology, National Cancer Institute, National Institutes of Health, Bethesda, Maryland 20014 and Department of Radiation Biology and Biophysics, University of Rochester, School of Medicine and Dentistry, Rochester, New York 14642

Received 29 October 1973; revised 1 July 1974

Summary. Ionophoric material isolated by tryptic digestion of $(Na^+ + K^+)$-ATPase containing electroplax membranes shows fluctuating discrete current levels in oxidized cholesterol membranes with conductance amplitudes ranging from 10^{-10} to 10^{-9} mhos, suggesting pore formation. The rate of pore formation is dependent on the imposed voltage. If the voltage is maintained for a short time (5 to 10 sec), pore formation is reversible, whereas permanent pores are formed when the voltage is maintained for more than 10 sec. At pH = 7 the permeability ratio for sodium versus chloride is 5 and for potassium versus sodium, 1.7. The permeability of the ionophoric material is dependent on pH. At pH = 6 a conversion takes place from more cation-permeable to more anion-permeable pores, suggesting that histidine plays a role in the permeation mechanism. A model is proposed to account for the observed ionophoric properties.

The initial stage of the conductance change induced in oxidized cholesterol bilayer membranes by a one-hour tryptic digest of $(Na^+ + K^+)$-ATPase containing electroplax membranes was voltage dependent (Shamoo & Albers, 1973) and showed properties similar to the properties of alamethicin-doped bilayer membranes (Mueller & Rudin, 1968). A 24-hour tryptic digest of the electroplax preparation provided active ionophoric material in greater yield and with properties similar to those of the one-hour tryptic digest with the notable exception that with the 24-hour tryptic digest the sodium dependent incorporation character was lost (Shamoo, Myers, Blumenthal & Albers, 1974).

In this paper we carry out further studies on the electrical properties of the 24-hour tryptic digest. We studied the kinetics of the voltage-dependent conductance change, ion selectivities and the mechanism of ion permeation by observing discrete fluctuations in current levels for a given voltage.

Previous studies with antibiotic ionophores established pore formation on the basis of discrete fluctuating current levels in the range of 10^{-11} to 10^{-9} mho for salt concentrations in the hundred millimolar range in the case of excitability-inducing material (EIM) (Bean, Shepard, Chan & Eichner, 1969; Ehrenstein, Lecar & Nossal, 1970), gramicidin (Hladky & Haydon, 1970) and alamethicin (Gordon & Haydon, 1972; Eisenberg, Hall & Mead, 1973). The amplitude of those conductance levels was considered too large to be accounted for by a carrier diffusing back and forth across the membrane. This consideration combined with the behavior of conductance levels as a function of voltage, salt concentration, solution viscosity and membrane thickness led to the conclusion that the above-mentioned ionophores induce pores in the membrane and that the opening of those pores gives rise to the conductance.

The data presented in this paper on discrete current fluctuations, the kinetics of voltage-dependent conductance change and ion selectivity together with the data presented by Shamoo and Albers (1973), Shamoo *et al.* (1974) and Shamoo and Myers (1974) on dose-response relationships and oligomerization led us to establish a model for the conductance induced by the ionophoric material in oxidized cholesterol bilayer membranes.

Materials and Methods

We used the 24-hour tryptic digest preparation, oxidized cholesterol and apparatus described by Shamoo *et al.* (1974). We added to the electronic circuit a wave form/sweep generator (Data Royal Model F230A) to generate voltage pulses and ramps and a Tektronix oscilloscope to measure the membrane time constant. The value of the membrane time constant was used to measure the membrane capacitance. Membrane thickness was derived from the capacitance, area (approximately 1 mm^2) and estimated dielectric constant (Fettiplace, Andrews & Haydon, 1971).

For the measurements of diffusion and biionic potentials a Teflon cup—hereafter referred to as inside chamber—was inserted into a plastic container—hereafter referred to as outside chamber. An outline of the top view of the outer chamber is that of two slightly overlapping equally sized circles with inner diameters equal to the outer diameter of the Teflon cup. The same solution volume of 3 ml added to the inside and outside chambers then produced equal levels of fluid in the two chambers.

The voltage source was switched to open circuit and the potential difference was measured with a Keithley electrometer. Two different procedures were applied: (1) The membranes are initially formed in a buffered solution with equal concentrations of K (or Na)Cl and subsequently small aliquots of 3 M Na (or K)NO_3 were added to one compartment. The potential was measured with Ag/AgCl electrodes. The advantage of this method is that there are no liquid junction potentials and that any initial potential difference due to asymmetry in the system can be detected from the start (Szabo, Eisenman & Ciani, 1969). (2) The membranes are initially formed in a buffer solution and subsequently small aliquots of potassium and sodium chloride, nitrate, sulfate or isethionate are added to the two different compartments. Calomel electrodes were used to measure

the potential. Fewer points are required to obtain the relevant parameters and measurements can be made in complete absence of chloride ion (Latorre, Ehrenstein & Lecar, 1972).

To avoid possible contributions of the ionophore concentration gradient to the diffusion potential, the ionophoric material was added to both solutions in those experiments. This is in contrast to the electrokinetic experiments (Fig. 1) where the ionophore was added to only one side. The parameters (P_{Cl}/P_{Na}) and (P_K/P_{Na}) are obtained by fitting the data to Eq. (3) by means of MLAB, an interactive computer (PDP-10) modeling system developed by the Division of Computer Research and Technology at the National Institutes of Health in Bethesda, Maryland.

Results

Current-Voltage Curves

We consider a positive current to be one in which cations flow from the inside to the outside chamber, and a positive voltage to be one where the potential of the inside chamber is more positive than that of the outside chamber.

When the ionophoric material is added to the inside chamber a conductance increase is observed only when the volltage is positive (Shamoo & Albers, 1973); with negative polarity a conductance increase will only be observed at higher concentrations of the ionophoric material and after longer times. Fig. 1*a* shows a typical current-votage curve measured at a voltage sweep rate of 6.2 mV/sec. The separation of the traces in the two different directions (indicated by arrows) is due to the capacitive charging current and is given by $i_c = C(dV/dt)$. Conductance below about 20 mV is indistinguishable from that of the black lipid without additive (bare membrane conductance is 4.0×10^{-8} mho/cm^2). The tryptic digest concentration in the inside chamber is 6.7×10^{-7} g/ml. The first leg of the sweep (starting from $V = 0$ going to the right in Fig. 1) is very similar to the I–V characteristic of alamethicin added to one side of a bilayer membrane (Mueller & Rudin, 1968; Eisenberg *et al.*, 1973).

The big difference between the current-voltage characteristic of alamethicin and that of the tryptic digest is that in the case of the tryptic digest the conductance does not return to baseline when the voltage is returned to zero. We see a hysteresis phenomenon: On the subsequent legs of the sweep the conductance is maintained at 10^{-9} mho.[1] A subsequent positive sweep will increase the conductance further until a steady-state conductance

1 We shall hereafter give conductance values in mho's rather than in the conventional mho/cm^2, because we are relating conductance changes to pore formation. The conductance per square centimeter can be obtained by dividing by the area of the membrane (0.01 cm^2).

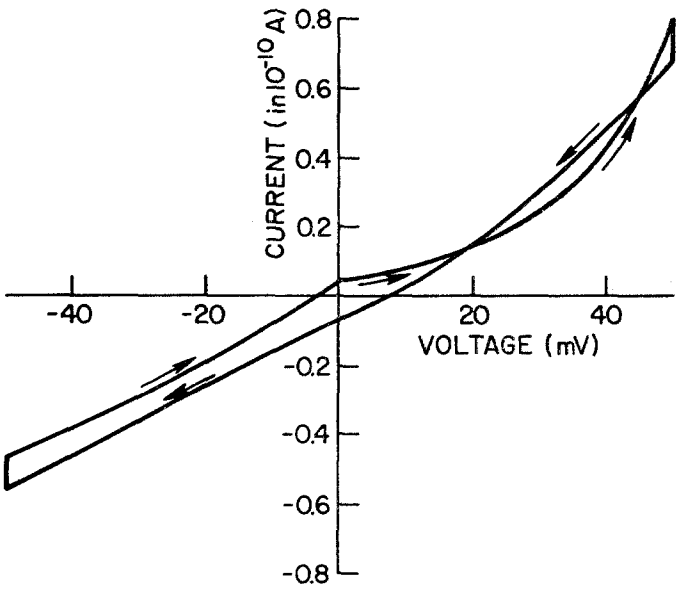

a

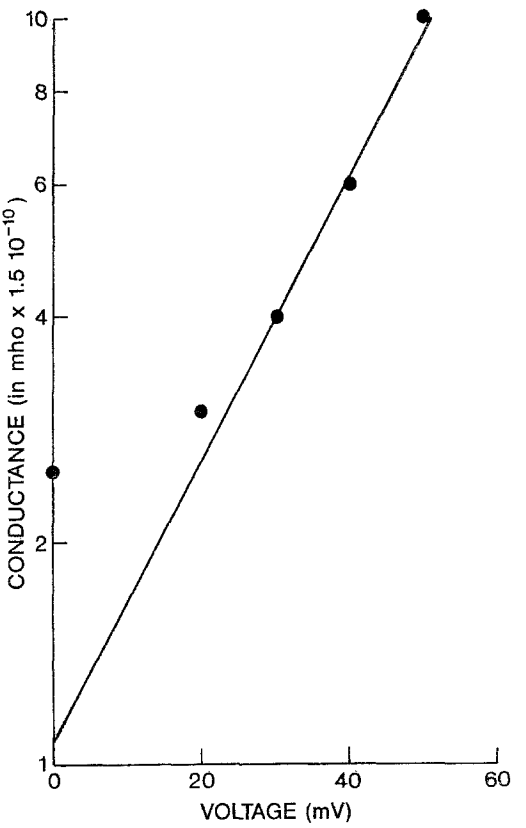

b

Fig. 1. (*a*) Voltage-current curve in symmetric 0.1 M NaCl with 6.7×10^{-7} g/ml of 24-hour tryptic digest added to the inside chamber. The arrows indicate the direction of the sweep ($dV/dt = 6.2$ mV/sec). (*b*) Conductance of the first leg of the sweep in Fig. 1 *a* plotted on a semi-logarithmic scale to show the exponential dependence of conductance on voltage

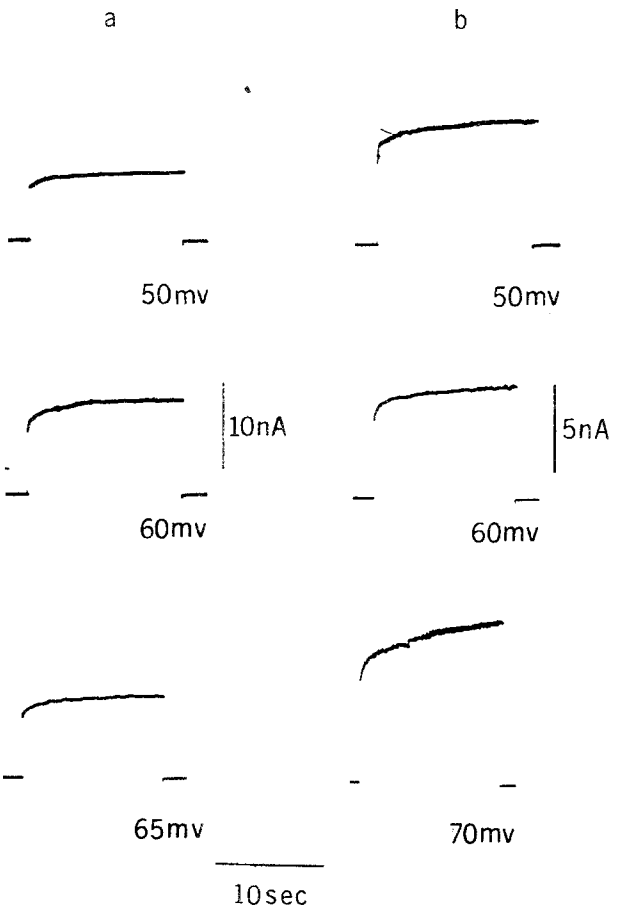

Fig. 2. Steady-state current driven by repetitive pulses (duration 13 sec, frequency 2 per min, voltage amplitude indicated by numbers). The sequence is from above downward. Symmetric 0.1 M NaCl; the concentration of 24-hour tryptic digest in the inside chamber was 6.7×10^{-7} g/ml in *a* and 1.3×10^{-7} g/ml in *b*

is reached. The positive voltage is needed to drive the pore-forming material over a voltage-dependent energy barrier.

Fig. 1*b* shows the conductance-voltage characteristic of the first leg of the current-voltage sweep of Fig. 1*a*, plotted in semi-logarithmic fashion. The voltage dependence is exponential and the conductance has the following form

$$G = G_o e^{aV} \tag{1}$$

where G is the conductance, V the voltage and a a measure of the steepness of the conductance change with voltage. From Fig. 1*b* we find $a = 0.05(\text{mV})^{-1}$.

Fig. 2 shows a series of consecutive pulses at a high conductance level (10^{-7} mho), obtained with 6.7×10^{-7} g/ml of 24-hour tryptic digest and

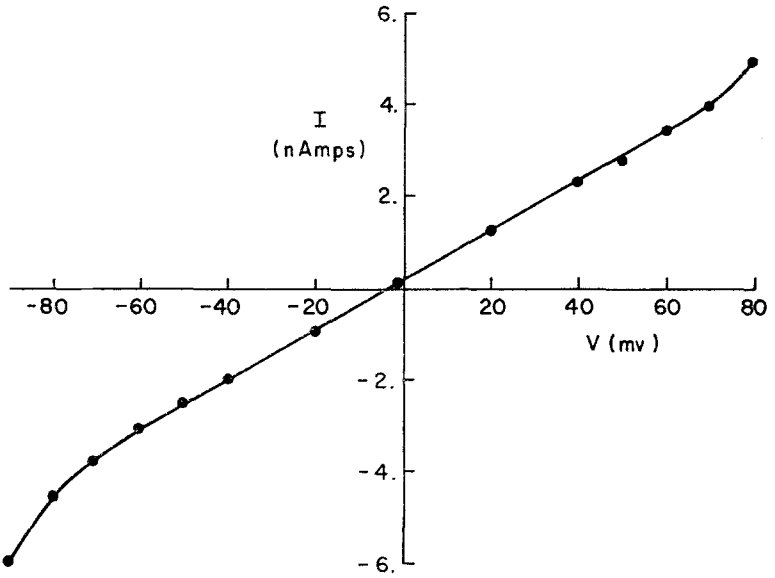

Fig. 3. Steady-state current measured at the end of a 13-sec voltage pulse (*see* Fig. 2) as a function of voltage in symmetric 0.1 M NaCl with 1.7×10^{-7} g/ml of 24-hour tryptic digest added to the inside chamber

0.1 M NaCl. Voltage pulses of given magnitude drive the current. The relation between the current at the beginning of the voltage pulse, "the instantaneous current", and the voltage is linear, indicating that the conductance is constant with time and that incorporation of the ionophore has reached a steady-state level. There remains, however, a very slight voltage-dependent component which increases the conductance by a factor of 1.4. A similar small voltage-dependent component has been observed with gramicidin A (Bamberg & Läuger, 1973) and has been related to a decrease in membrane thickness due to a compressive force exerted by the electric field. A nearly linear current-voltage curve for a different membrane (1.7×10^{-7} g/ml of 24-hour tryptic digest, 0.1 M NaCl) is shown in Fig. 3 obtained by imposing d-c voltage pulses and measuring the steady-state current at the end of a 13-sec pulse as shown in Fig. 2.

Discrete Current Levels

We have seen that a voltage-induced conductance increase cannot be returned to baseline upon removing the imposed voltage, if the voltage is imposed for over 10 sec either by a ramp as in Fig. 1 or by a d-c pulse. To observe current fluctuations we applied voltage pulses lasting 13 sec.

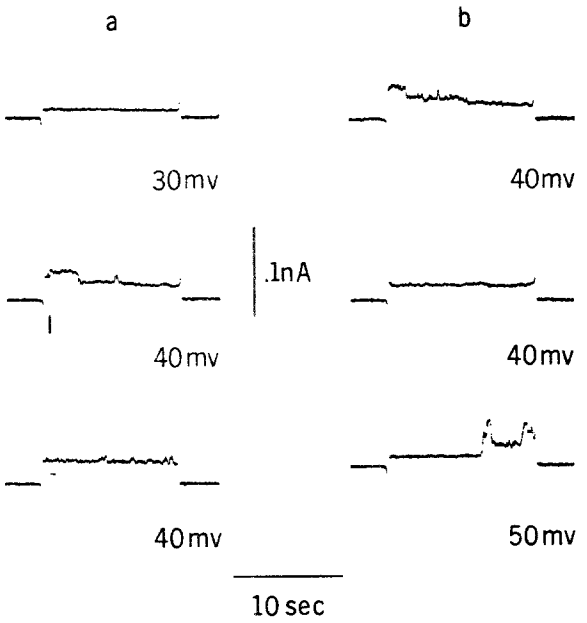

Fig. 4. Current driven by repetitive pulses (duration 13 sec, frequency 2 per min, voltage amplitude indicated by numbers). The sequence is from above downward. Symmetric 0.1 M NaCl;* 1.3×10^{-7} g/ml of 24-hour tryptic digest in the inside chamber. There is a 1-min time interval between the series of pulses in parts *a* and *b*

Conductance increases occur in 5 to 10 sec after the beginning of the pulse and those increases are returned to baseline upon removal of the imposed voltage within the remaining 3 to 8 sec.

Figs. 4 and 5 show a series of consecutive current pulses from top to bottom at 17-sec intervals driven by 13-sec voltage pulses of indicated magnitude. The 24-hour tryptic digest is added to the inside chamber only at a concentration of 1.3×10^{-7} g/ml. The first pulse in Fig. 4*a* shows the baseline current of the black lipid membrane without additive and a conductance of 3.3×10^{-10} mho. The second pulse shows a short-lived current fluctuation ($\Delta G = 2.5 \times 10^{-10}$ mho) followed by a fluctuation ($\Delta G = 3.7 \times 10^{-10}$ mho) lasting 3 sec. The third pulse shows fluctuations ($\Delta G = 2.5 \times 10^{-10}$ mho) on top of the background current of the membrane with some additive ($G = 6.2 \times 10^{-10}$ mho).

Fig. 4*b* represents current fluctuations on the same membrane after a time interval of 1 min. The conductance has returned back to baseline

* Although the experiments presented in Fig. 2*b* and 4 were carried out under the same experimental conditions they represent different levels of incorporation of the ionophore. The tracings in Fig. 2*b* were obtained after the membrane was subjected to voltage pulses for over 30 min.

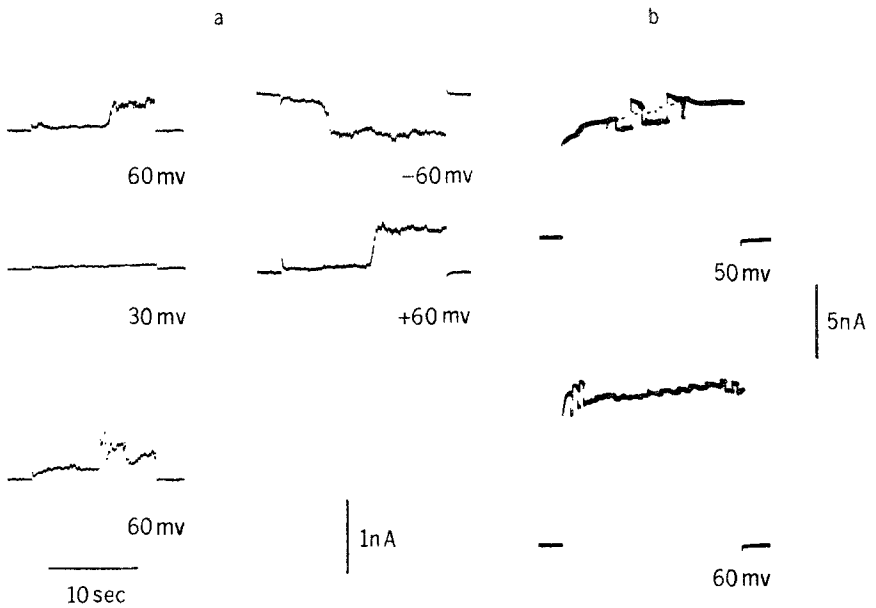

Fig. 5. Current driven by repetitive pulses (duration 13 sec, frequency 2 per min, voltage amplitude indicated by numbers). The sequence is from above downward starting from the left side. Symmetric 0.1 M NaCl; 1.3×10^{-7} g/ml of 24-hour tryptic digest in the inside chamber. There is an interval of about 10 min between the series of pulses in parts *a* and *b*, during which the repetitive stimulation was continued at the same frequency. Fig. 5*b* represents a higher conductance level

level (first pulse); after 6 sec the first fluctuating level ($\Delta G = 2.5 \times 10^{-10}$ mho) appears followed by a larger fluctuation ($\Delta G = 4 \times 10^{-10}$ mho). During the second pulse in Fig. 4*b* the 4×10^{-10} mho level has disappeared, whereas during the third pulse two fluctuating current levels ($\Delta G = 3.7 \times 10^{-10}$ mho) appear. The amplitudes of conductance levels shown in Fig. 4 are in the range of amplitudes observed in EIM (Bean *et al.*, 1969; Ehrenstein *et al.*, 1970) and alamethicin (Gordon & Haydon, 1972; Eisenberg *et al.*, 1973).

Because we run into the problem of permanent conductance changes if we maintain the voltage for over 10 sec after the conductance increase we do not have enough data on current fluctuations to carry out statistics on conductance level distributions (Eisenberg *et al.*, 1973) or dwell times for open pores (Ehrenstein *et al.*, 1974). The dwell times in Fig. 4 between 1 and 3 sec are in the range of the average dwell times of EIM pores in oxidized cholesterol (Ehrenstein *et al.*, 1974). We also observed the current fluctuations with the appropriate conductance changes when voltage ramps were applied to drive the current.

Fig. 5 shows larger current fluctuations on the same membrane as in Fig. 4. The conductance level is 5×10^{-9} mho, which corresponds to the fourth conductance level of alamethicin in 1 M NaCl (Eisenberg *et al.*, 1973). In addition to a voltage-induced conductance increase, which is permanent, we note another difference from alamethicin: In the case of alamethicin the higher conductance levels are only obtained gradually by passing through the lower levels, whereas, in our case the high level bursts occur independently of previous conductance increases.

Fig. 5*a* shows five consecutive pulses at 17-sec intervals starting from the left row going downwards with 1.3×10^{-7} g/ml of 24-hour digest added to the inside chamber in the presence of 0.1 M NaCl. Conductance increase induced by a 60-mV pulse (first row) is reversible; the voltage is only maintained 3 sec after the conductance increase. The subsequent 30-mV pulse shows only baseline current. We have seen from Fig. 1 that the probability of conductance increase at 30 mV is much less than the probability at 60 mV. A subsequent 60-mV pulse reinduces the conductance. Originally the material was only added to the inside chamber and only a positive voltage induced conductance increase. In at least 20 experiments we maintained the voltage at -50 mV for over 10 min and did not observe a conductance change. When the voltage was subsequently switched to $+50$ mV a conductance change occurred within 1 min. The peptides producing the conductance increase can in principle return to the membrane-solution interface on *either* side of the membrane upon relaxation of the voltage during the reversible stage of conductance increase.

This is what we see in Fig. 5*a*: The first column, third row, shows that a conductance has been induced by a 60-mV positive voltage pulse. After a 17-sec interval we apply a 60-mV *negative* pulse (second column, first row). From the low initial current during that negative pulse we infer that the conductance induced by the previous pulse had disappeared. If ionophoric material were only adsorbed on the inside membrane-solution interface the negative pulse would not reinduce the conductance. The appearance of the large current level during the negative pulse indicates that the material producing the conductance increase comes from the outside interface.

Fig. 5*b* shows current fluctuations ($\Delta G = 10^{-9}$ mho) in a high conductance (5×10^{-7} mho) membrane.

The Kinetics of Conductance Change

The experiment of Fig. 1 indicates that the activation energy to form pores has a voltage-dependent component. To take a closer look at the

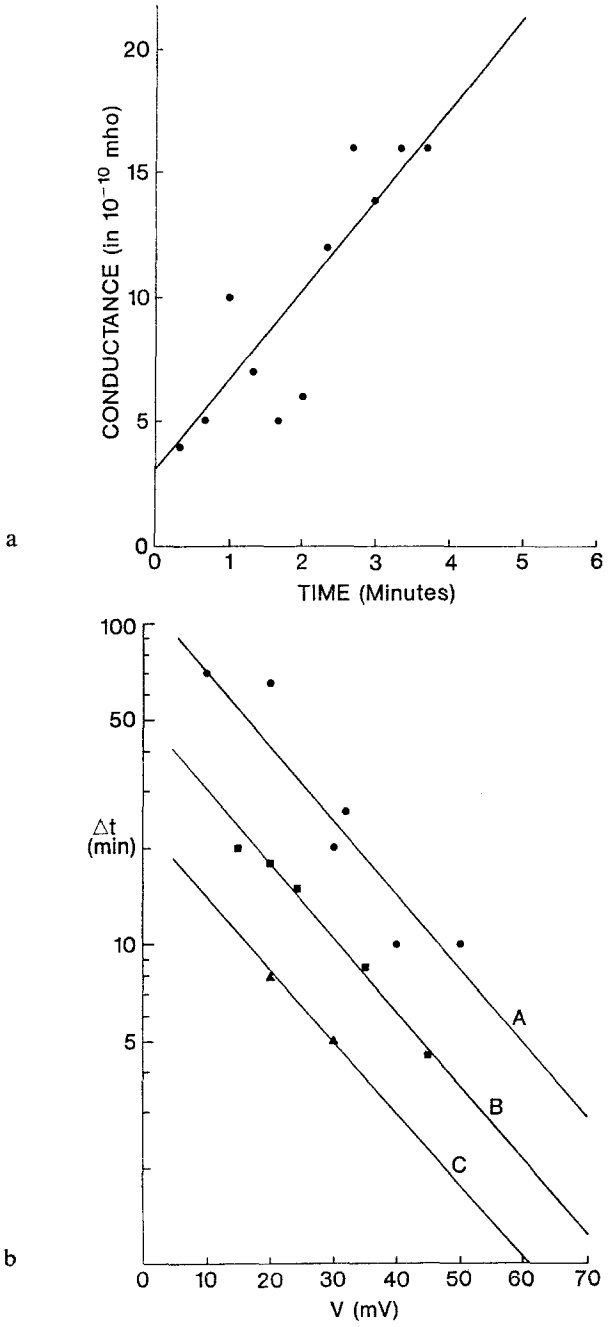

Fig. 6. (*a*) Development of the conductance change in an oxidized cholesterol membrane with symmetric 0.1 M NaCl and 6.7×10^{-7} g/ml of tryptic digest in the inside chamber. The imposed voltage is 45 mV. (*b*) The time Δt to reach a given conductance level (210^{-9} mho) plotted on a semi-logarithmic scale as a function of imposed voltage V. Each point represents a different membrane at a given voltage and a given concentration of ionophoric material. The three lines represent three different 24-hour tryptic digest concentrations in the inside chamber: (*A*) 6.7×10^{-8} g/ml, (*B*) 6.7×10^{-7} g/ml, (*C*) 3.3×10^{-6} g/ml; symmetric 0.1 M NaCl

voltage dependence, we measured the time required to establish a given conductance level as a function of the voltage. The implicit assumption is that initially G is a linear function of time. In Fig. 6*a* we replotted G as a function of time from the original record – monitored by a pen recorder – at $V = 45$ mV with 1.3×10^{-7} mg/ml of 24-hour digest in the inside chamber and 0.1 M NaCl on both sides. The spread in the points in Fig. 6*a* is a manifestation of formation of bumps as shown in Figs. 4 and 5. On the average, however, the conductance increases linearly with time as indicated by the solid line.

For experiments with much slower time courses of the conductance change we did not monitor the time course but took the time interval Δt for which the conductance had reached a given value of $G = 2 \times 10^{-9}$ mho. The latter value is about 10 times the bare membrane conductance, but far below the steady-state conductance ($G = 10^{-7}$ to 10^{-6} mho) for the tryptic digest concentration used in the kinetic experiments. We therefore were confident that we were carrying out our Δt measurements in the linear range of G versus time.

Fig. 6*b* shows the results for three different 24-hour tryptic digest concentrations where Δt is plotted in a semilogarithmic fashion as a function of imposed voltage. The voltage dependence is exponential and has the following form:

$$\Delta t = \Delta t_o e^{-aV}. \tag{2}$$

In Eq. (2), a is a measure of the steepness of the *rate of conductance change* with voltage. We find $a = 0.05$/mV, the same value for a as found by the ramp experiment in Fig. 1. This finding does not surprise us because with the voltage sweep we are also measuring the rate of conductance change.

Ion Selectivities

In Figs. 7 and 9 diffusion and biionic potentials are plotted against the logarithm of cation concentration ratios. The data are fitted to the Goldman-Hodgkin-Katz equation (*see* Hodgkin & Katz, 1949):

$$V = -\frac{RT}{F} \ln\left((\mathrm{Na}_i + (P_\mathrm{K}/P_\mathrm{Na})\,\mathrm{K}_i + (P_\mathrm{Cl}/P_\mathrm{Na})\,\mathrm{Cl}_o)/(\mathrm{Na}_o + (P_\mathrm{K}/P_\mathrm{Na})\,\mathrm{K}_o + (P_\mathrm{Cl}/P_\mathrm{Na})\,\mathrm{Cl}_i)\right) \tag{3}$$

where Na, K, Cl and P_Na, P_K and P_Cl are, respectively, the concentrations and permeability constants of sodium, potassium and chloride. The sub-

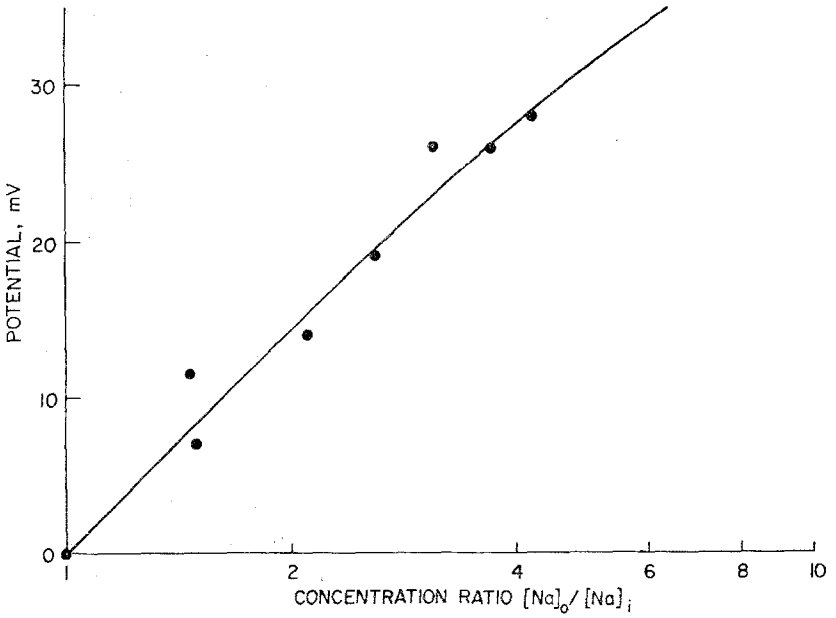

Fig. 7. The diffusion potential plotted as a logarithmic function of the ratio of concentrations of sodium chloride in the outside and inside chambers. The concentration of 24-hour tryptic digest in both chambers was 6.7×10^{-8} g/ml, at pH = 7 and membrane conductance 2×10^{-9} mho. The points represent data and the solid line is calculated from Eq. (3) with $P_{Cl}/P_{Na} = 0.1$

scripts *i* and *o* refer to the inner and outer chamber, respectively. *R*, *T* and F are, respectively, the gas constant, temperature and the Faraday constant. With Ag/AgCl electrodes, nitrate is the abundant anion (*see* Materials and Methods); in that case the NO_3^- permeability is assumed to equal Cl^- permeability.

Curve fitting of the data presented in Fig. 7 to Eq. (3) yields $P_{Cl}/P_{Na} = 0.1$. At pH = 7 we find that P_{Cl}/P_{Na} runs between 0.1 and 0.8 for 20 tryptic digest batches with low and high conductance membranes. In other words, at pH = 7.0 the tryptic digest-doped membrane is more permeable to monovalent cations than to monovalent anions. This seems paradoxical because the voltage-dependent incorporation data indicate a positive charge on the ionophore. A similar situation was obtained by Cass, Finkelstein and Krespi (1970) in the case of positively charged polyene antibiotics, by Muller and Finkelstein (1973) in the case of monazomycin, and by Eisenberg *et al.* (1973) in the case of alamethicin. To obtain a situation in which the ionophore totally excludes anions we measured diffusion potentials using sodium sulfate.

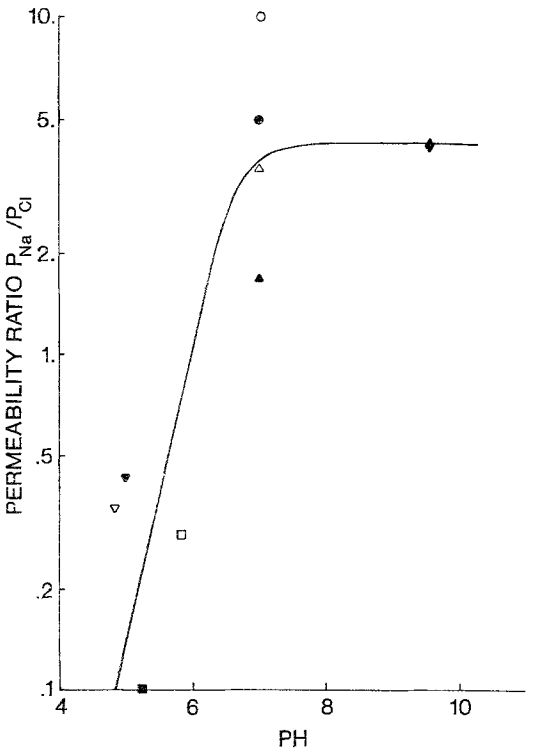

Fig. 8. The sodium-to-chloride permeability ratios, obtained by measuring diffusion potentials as a function of sodium concentration ratios as shown in Fig. 7 and by fitting the data to Eq. (3), as a function of pH. The different points represent separate experiments with tryptic digest concentrations 6.7×10^{-8} to 1.7×10^{-7} g/ml and membrane conductance ranging from 10^{-9} to 10^{-8} mhos. The experiments represented by ○, ●, △, ▲ were carried out in histidine buffer; by ♦ in tris buffer; by ▽ in ammonium acetate buffer; by ▼, □ and ■ in the absence of buffer; in the latter case the pH was measured before and after the experiment

It is not meaningful to fit those data to the Goldman-Hodgkin-Katz equation (3), because of the divalent sulfate ion. The slope of the voltage versus the logarithm of the sodium activity ratio was 50 to 53 mV/decade in the case of SO_4^{2-} compared with 40 mV/decade in the case of Cl^- or NO_3^-. Although the ionophore is, as expected, more impermeable to divalent anions than to monovalent anions, pure cation selectivity which would produce a slope of 59 mV/decade is not obtained. Sodium isethionate which is a larger monovalent anion also produces a slope of 50 mV/decade. The activity coefficients are, however, not known in the latter case.

Fig. 8 shows P_{Na}/P_{Cl} as a function of pH obtained by measuring the diffusion potential as a function of salt concentration at various pH's and calculating P_{Na}/P_{Cl} from Eq. (3) using the curve-fitting routine. The sur-

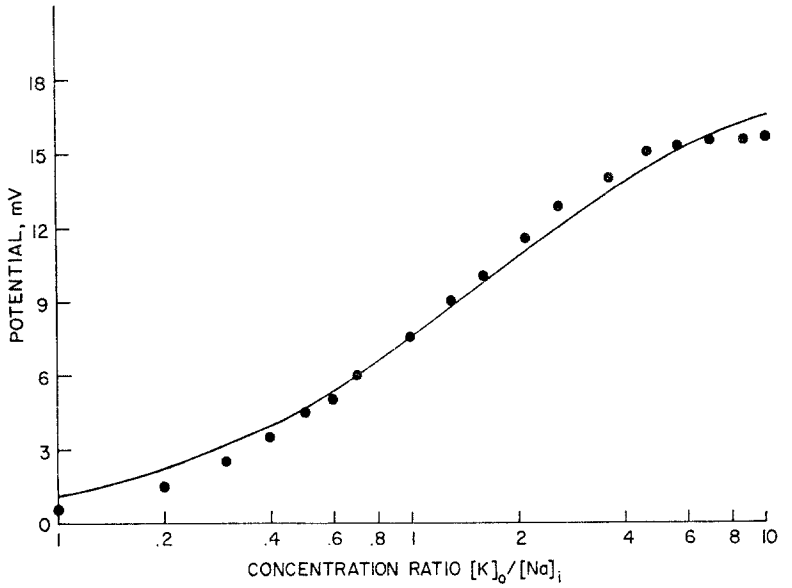

Fig. 9a

Fig. 9. Biionic potentials plotted as a logarithmic function of potassium-to-sodium concentration ratios. The subscripts *i* and *o* indicate inside and outside concentration ratios, respectively. (*a*) In both chambers the 24-hour tryptic digest concentration was 2.3×10^{-7} g/ml and the initial NaCl concentration was 0.01 M. The potential was measured with Ag/AgCl electrodes; KNO_3 was added to the outside chamber at pH = 7 and conductance 9×10^{-9} mho. The points represent data and the solid line is calculated from Eq. (3), with $P_{Cl}/P_{Na} = 0.8$ and $P_K/P_{Na} = 1.7$. (*b*) In both chambers the 24-hour tryptic digest concentration was 3.3×10^{-7} g/ml and the initial histidine chloride concentration was 0.005 M. Equal amounts of potassium and sodium chloride were then added to the inside and outside chambers, respectively. The potential was measured with calomel electrodes, at pH = 7 and membrane conductance 5×10^{-9} mho. The points represent data and the solid line is calculated from Eq. (3) with $P_{Cl}/P_{Na} = 0.3$ and $P_K/P_{Na} = 1.9$

prising result is the conversion at pH = 6 from a cation- into an anion-selective ionophore. Even at high pH (9.6) the ionophore does not become purely cation selective; i.e., even when the charge is negative the pore is large enough to accommodate anions. We have not carried out the experiments to sufficiently low pH's to find "saturation" of P_{Na}/P_{Cl}. The inversion point where cations and anions are equally permeable is at pH = 6. This is consistent with a titratable histidine group on the ionophore. The latter is contradicted by the photooxidation experiments of Shamoo *et al.* (1974). The 0.1% methylene blue photooxidation causing the inactivation of 80% of the ionophoric material was namely pH independent. The conversion from cation selectivity to anion selectivity when the pH of the bathing fluid

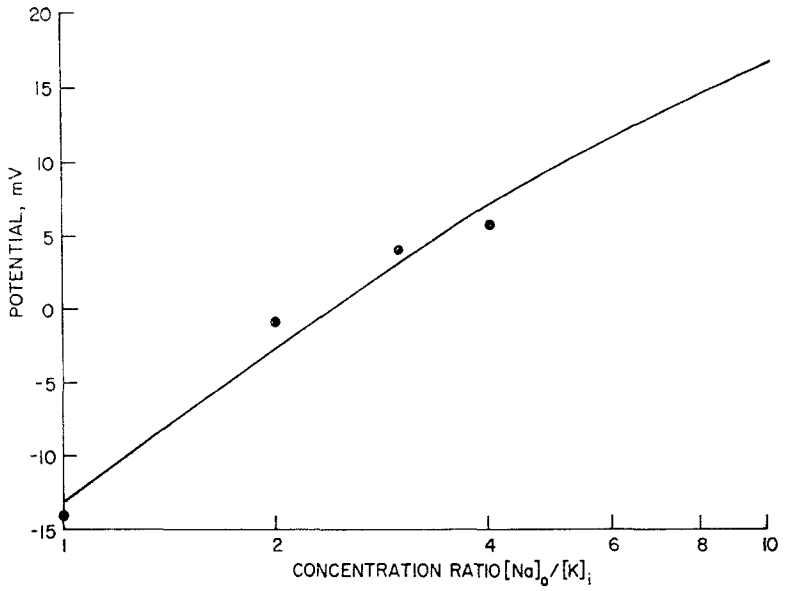

Fig. 9b

is below 6.0, has also been observed in the gallbladder membranes by Diamond and Wright (1969).

Potassium-to-sodium permeability ratios are obtained from data shown in Fig. 9*a* and *b*. From fitting the data of Fig. 9*a* to Eq. (3) we obtain $P_{Cl}/P_{Na} = 0.8$ and $P_K/P_{Na} = 1.7$ and the data in Fig. 9*b* yield $P_{Cl}/P_{Na} = 0.3$ and $P_K/P_{Na} = 1.9$. The range of those values has been obtained consistently with 15 tryptic digest batches and at varying membrane conductances. The formed pores show the same selectivity for potassium over sodium as their mobility ratio in aqueous solution. Similar results have been obtained with EIM (Latorre *et al.*, 1972) and alamethicin (Eisenberg *et al.*, 1973) which form nonspecific pores.

The permeability of the ionophore to anions is another indication of pore formation because to our knowledge no carriers have hitherto been found which deviate from pure cation selectivity.

Discussion

We propose the following scheme for the conductance change induced by the tryptic digest in oxidized cholesterol membranes.

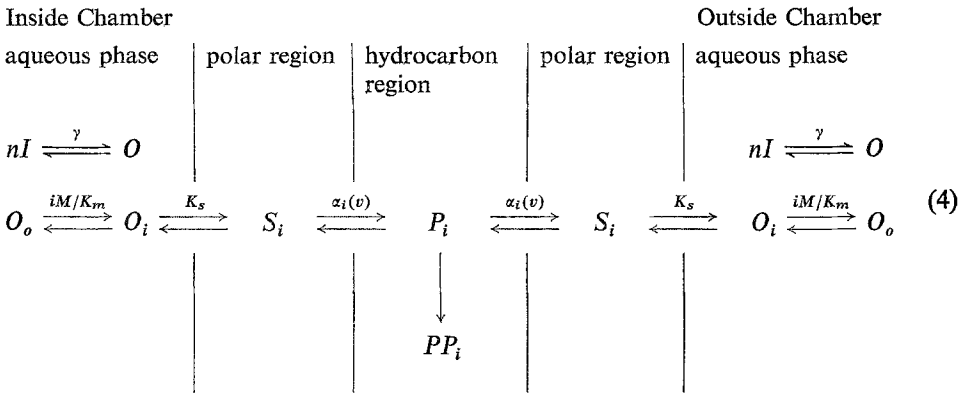

(4)

When we add the ionophoric material, which was stored for five days at 0.2 mg/ml and pH = 2, to the inside chamber at pH = 7 we find no activity (Shamoo *et al.*, 1974). We interpreted this experiment in terms of oligomerization; at pH = 2 the oligomers are disaggregated into monomers which are inactive. When we subsequently store the material for five days at 0.2 mg/ml and at pH = 7 we can restore the ionophoric activity.

These findings indicate that first the monomers have to reaggregate in *aqueous solution* before they can adsorb to the membrane. The aggregation process occurs at a rate of over 24 hr which is much longer than the duration of the experiment (10 to 60 min). If monomers could adsorb to the membrane and form aggregates on the membrane (as apparently occurs in the case of alamethicin) we would find immediate activity at pH = 7 after storing at pH = 2 to 3. The assumption that only oligomers will adsorb to the membrane is plausible in view of the fact that, generally, aggregates are less water soluble and tend to aggregate.

In the storage solution an aggregation equilibrium is established, which is the same as in the inside chamber, to which the material is applied, except for a dilution factor (volume of an aliquot of the storage solution/ volume of the solution in the inside chamber):

$$O = \gamma I^n \tag{5}$$

where O is the oligomer concentration, γ the aggregation constant, I the monomer concentration and n the number of monomers in the oligomer.[2]

In the presence of monovalent cations a complex formation takes place with a binding site on each monomer probably made up of peptide carbonyl

2 O and I only refer to the concentrations of oligomer and monomer which are potential pore formers. Because the sample is impure it is a small fraction of the total added material.

groups. In the case of the one-hour tryptic digest the dissociation constant for sodium is much lower than for the other monovalent cations (Shamoo & Albers, 1973). Generally, complex formation rates of monovalent cations to ionophores are very fast: 10^{-9} sec in the case of monactin (Eigen & DeMaeyer, 1971). The concentration of oligomer in the inside chamber with i ions bound (*see* the section on linked functions in Wyman, 1948) is given by:

$$O_i = \binom{n}{i} (M/K_m)^i O/(1+M/K_m)^n \tag{6}$$

where M represents monovalent cation concentration, K_m the dissociation constant of the complexed binding site and O the total concentration of oligomer, which equals the amount of oligomer initially added to the inside chamber. For simplicity we assume no interaction between binding sites (they all have the same K_m) and the number of binding sites n equals the number of monomers per oligomer.

The absorption equilibrium to the polar region is determined by the constant K_s, and S_i is the concentration of oligomer complexed with i cations at the interface. Ion binding may also occur at the interface; we assume the same dissociation constant for the adsorbed complex (S_i), as for the complex in solution (O_i). The time constant for adsorption from solution to the bilayer interface is 2.9 min in the case of alamethicin (Eisenberg *et al.*, 1973).

The voltage-dependent transition $S_i \rightleftarrows P_i$ leads to the formation of ion-conducting pores with voltage-dependent formation rate constant $\alpha_i(v)$. We assume this step to be rate-limiting; for $V = 45$ mV the time constant is certainly larger than 10 min.

We see a considerable heterogeneity of single conductance events ranging from 10^{-10} to 10^{-9} mho. We assume that the heterogeneity is a reflection of different pore sizes determined by the number of charges i on the pore.

The step $P_i \rightarrow PP_i$, where PP_i indicates permanent pore with charge i has a time constant of 5 to 10 sec according to the experiments presented in Figs. 1 and 4. If the voltage is maintained for less than 5 sec the pore will disappear after removal of the voltage, causing a $P_i \rightleftarrows S_i$ transition either to the inside or outside surface of the bilayer (*see* Fig. 5). After maintaining the voltage, however, for a longer period the pore cannot be removed by relaxing the voltage. Steady-state conductance (which is independent of voltage) will be reached when all the oligomer in solution is used up and converted to permanent pore. It is essentially a quasi steady state because upon removal of oligomer from solution further aggregation of monomers

into oligomers will take place. The time constant for that process (24 hr) is, however, much larger than the duration of an experiment (10 to 60 min) so that we can neglect aggregation during the experiment. The steady-state conductance is given by

$$G = \sum_{i=1}^{n} g_i PP_i \tag{7}$$

where g_i is the conductance of a pore with charge i. We assume g_i to be the same for a reversible or permanent pore; the magnitude is determined by the charge on the oligomer. The total amount of permanent pore with charge i at steady state is given by

$$PP_i = vAO_i \tag{8}$$

where v is the volume of the chamber and A the avogadros number.

Substituting for PP_i according to Eq. (8) and for O_i according to Eqs. (5) and (6) into Eq. (7) yields

$$G = vA\gamma I^n \sum_{i=0}^{n} \binom{n}{i} g_i (M/K_m)^i / (1 + M/K_m)^n. \tag{9}$$

Eq. (9) accounts for the higher order dependence of the conductance on concentration of the ionophoric material as shown by Shamoo and Albers (1973) and for the dependence on monovalent ion concentration as shwon by Shamoo *et al.* (1974).

We can illustrate, by a numerical example, the range of oligomer concentration and consequently the amount of permanent pores in the membrane at steady state. Making use of Eqs. (8) and (5) we derive the total amount of permanent pore at steady state

$$PP_t = \sum_{i=1}^{n} PP_i = vA \sum_{i=1}^{n} O_i = vAO = vA\gamma I^n. \tag{10}$$

If we take $I_t = 10^{-7}$ mole, $n = 6$ and $\gamma = 10^{25}/(\text{mole})^{n-1}$ we obtain from Eq. (5) $O = 10^{-17}$ mole. The total amount of material added to the inside chamber then equals $I + O \approx I$. From Eq. (10) we obtain $PP_t = 10^3$ permanent pores. With an average permanent pore conductance of 5×10^{-9} mho, we arrive at a total membrane conductance of 5×10^{-6} mho.

The initial rate of conductance change is determined by the rate-limiting step $S_i \rightarrow P_i$ in Eq. (4) and given by

$$\frac{dG}{dt} = \sum_{i=1}^{n} g_i \frac{dP_i}{dt} = \sum_i g_i \alpha_i(V) S_i. \tag{11}$$

The rate constant $\alpha_i(V)$ is determined by an activation energy between the peptides absorbed on the membrane and the peptides forming the pore. The activation energy has a voltage-dependent component and therefore the rate constant can be decomposed according to (Mueller & Rudin, 1968; Eisenberg *et al.*, 1973; Muller & Finkelstein, 1973; Ehrenstein *et al.*, 1974):

$$\alpha_i(V) = \alpha_i(o)\, e^{a_i V} \tag{12}$$

where $\alpha_i(o)$ is the rate constant in the absence of an imposed voltage and a_i the steepness of the voltage-dependent rate constant for the formation of an i^{th} level pore. We define an average steepness a by

$$e^{aV} = \frac{\sum_{i=1}^{n} g_i \alpha_i(o)\, S_i\, e^{a_i V}}{\sum_{=1}^{n} g_i \alpha_i(o)\, S_i} = \frac{(dG/dt)}{(dG/dt)_{V=0}}. \tag{13}$$

We replace the differential in Eq. (13) by the difference ($dG/dt = \Delta G/\Delta t$), because we consider the linear range of conductance change with time. We then eliminate ΔG in Eq. (13), because we consider the time required to obtain a *given* conductance change ($\Delta G = (\Delta G)_{V=0} = 2 \times 10^{-9}$ mhos) as a function of voltage. Eq. (13) then reduces to Eq. (2).

Two types of physical interpretations have been invoked for the parameter a (Ehrenstein *et al.*, 1974): (1) When a charge is moved by the field across the membrane, the peptides form a pore. One can deduce how many charges have to be moved. From the value we measured ($a = 0.05\ \text{mV}^{-1}$) we derive an average of one charge. (2) A change in dipole moment between the adsorbed peptides and the pore peptides occurs during pore formation. From the value of a, we obtain a change in dipole moment of 300 debye.

We believe that permanent pore formation occurs because the peptides that form a bridge across the membrane interact with peptides that have formed a "bridge head" on the other side of the membrane. The complex of the "bridge" and the "bridge head" cannot be removed upon relaxation of the voltage. If the voltage is only maintained for 5 to 10 sec there is not enough time for the "bridge" and "bridge head" to form a stable complex. This idea is consistent with the observation that the rate pore formation is much faster when the same amount of material is applied to both sides of the membrane: In the latter case the "bridge heads" do not have to be transported across the membrane prior to forming the stable complexes because they are already present on both sides. Our observation (Shamoo

et al., 1974) that by application of the ionophoric material to both sides of the membrane, the same steady-state conductance level can be attained with a 50- to 200-fold reduction in the amount of added material, is explained by assuming that only 0.5 to 2% of the "bridge heads" are permeable through the membrane.

Conclusion

We have described the properties of a very interesting ionophore (or ionophores) released by a tryptic digest from electroplax membranes. We have studied the ionophore as if it were any other of the known antibiotic ionophores without relating it to any physiological function.

The question as to why the ionophoric material does not produce conductance changes in lipid bilayer membranes made up of lecithin, lipid extracts from electric organ or even mixtures of brain phospholipids and cholesterol still need elaboration.

The electroplax membrane is rich in ionophores necessary for synaptic function, spike electrogenesis and for maintaining the ionic (K^+, Na^+) concentration gradients (Changeux, Podleski, Kasai & Blumenthal, 1970). The synaptic ionophores are associated with the acetylcholine receptor; the spike-generating mechanism is made up of voltage-dependent sodium and potassium channels; and the ionic balance is maintained by the ($Na^+ + K^+$)-ATPase active transport system. We can estimate the relative abundance of ($Na^+ + K^+$)-ATPase and other channels in the electroplax membrane preparations. Albers, Koval and Siegel (1968) measured 1000 nmoles ($Na^+ + K^+$)-ATPase/g protein on the basis of ^{32}P incorporation, whereas Changeux and his co-workers (Changeux, Kasai & Lee, 1970; Olsen, Meunier & Changeux, 1972) measured 1 nmole acetylcholine receptor/g protein in electroplax membrane preparation on the basis of radioactive labeled α-bungarotoxin binding. Conductance measurements on the isolated electroplax cell (Ruiz-Manresa & Grundfest, 1971) show that the amount of synaptic (acetylcholine receptor) channels is about the same as electrically excitable channels. The latter will then also be in the 1 nmole/g protein range. If we therefore subject the membrane preparations to a tryptic digestion the chances are 1000 to 1 that the released ionophoric material is derived from ($Na^+ + K^+$)-ATPase.

To prove that contention, we are carrying out further studies on the purification of the active ionophore and on the possible reconstitution of permeability gating with ATP.

It is a pleasure to acknowledge our debt to Dr. William T. Adelman, Jr. for generously providing the facilities at the Laboratory of Biophysics, NINDS, NIH, where the biophysical measurements were carried out; to Dr. R. Wayne Albers for generously providing the facilities at the Laboratory of Neurochemistry, NINDS, NIH, where the samples of the tryptic digest of eel electroplax were prepared; to Marjory Myers for preparation of the samples; and to Dr. Harold Lecar for his valuable comments throughout the course of this work.

This paper was based on work partially performed under contract with the U.S. Atomic Energy Commission at the University of Rochester Atomic Energy Project and has been assigned Report No. UR-3490-407. The work was also supported in part by NSF Grant No. GB-40657.

References

Albers, R. W., Koval, G. J., Siegel, G. J. 1968. Studies on the interaction of ouabain and other cardioactive steriods with sodium-potassium-activated adenosine triphosphatase. *Mol. Parmacol.* **4**:324

Bamberg, E., Läuger, P. 1973. Channel formation kinetics of gramicidin A in lipid bilayer membranes. *J. Membrane Biol.* **11**:177

Bean, R. C., Shepherd, W. C., Chan, H., Eichner, J. T. 1969. Discrete conductance fluctuations in lipid bilayer protein membranes. *J. Gen. Physiol.* **53**:741

Cass, A., Finkelstein, A., Krespi, V. 1970. The ion permeability in thin lipid membranes by the polyene antibiotics nystatin and amphotericin. *J. Gen. Physiol.* **56**:100

Changeux, J.-P., Kasai, M., Lee, Ch-Y. 1970. Use of a snake venom toxin to characterize the cholinergic receptor protein. *Proc. Nat. Acad. Sci.* **67**:1241

Changeux, J.-P., Podleski, T., Kasai, M., Blumenthal, R. 1970. Some molecular aspects of membrane excitation studied with eel electroplax. *In*: Excitatory Synaptic Mechanisms. P. Anderson and J. J. Jensen, editors. p. 123. University Press, Oslo

Diamond, J. M., Wright, E. M. 1969. Biological membranes: The physical basis of ion and nonelectrolyte selectivity. *Annu. Rev. Physiol.* **31**:581

Ehrenstein, G., Blumenthal, R., Latorre, R., Lecar, H. 1974. The kinetics of the opening and closing of individual EIM channels in a lipid bilayer. *J. Gen. Physiol.* **63**:707

Ehrenstein, G., Lecar, H., Nossal, R. 1970. The nature of the negative resistance in bimolecular lipid membranes containing excitability-inducing material. *J. Gen. Physiol.* **55**:119

Eigen, M., DeMaeyer, L. 1971. Carriers and specificity in membranes. *Neurosci. Res. Prog. Bull.* **9**:300

Eisenberg, M., Hall, J. E., Mead, C. A. 1973. The nature of the voltage-dependent conductance induced by alamethicin in black lipid membranes. *J. Membrane Biol.* **14**:143

Fettiplace, R., Andrews, D. M., Haydon, D. A. 1971. The thickness, composition and structure of some lipid bilayers and natural membranes. *J. Membrane Biol.* **5**:277

Gordon, L. G. M., Haydon, D. A. 1972. The unit conductance channel of alamethicin. *Biochim. Biophys. Acta* **255**:1014

Hladky, S. B., Haydon, D. A. 1970. Discreteness of conductance change in bimolecular lipid membranes in the presence of certain antibiotics. *Nature* **255**:451

Hodgkin, A. L., Katz, B. 1949. The effect of sodium ions on the electrical activity of the gaint axon of the squid. *J. Physiol.* **108**:37

Latorre, R., Ehrenstein, G., Lecar, H. 1972. Ion transport through excitability-inducing material (EIM) channels in lipid bilayer membranes. *J. Gen. Physiol.* **60**:72

Mueller, P., Rudin, D. O. 1968. Action potentials induced in bimolecular lipid membranes. *Nature* **217**:713

Muller, R. U., Finkelstein, A. 1973. Voltage-dependent conductance induced in thin lipid membranes by monazomycin. *J. Gen. Physiol.* **60**:263

Olsen, R. W., Meunier, J.-C., Changeux, J.-P. 1972. Progress in the purification of the cholinergic receptor protein from electrophorus electricus by affinity chromatography. *FEBS Letters* **28**:96

Ruiz-Manresa, F., Grundfest, H. 1971. Synaptic electrogenesis in eel electroplaques. *J. Gen. Physiol.* **57**:71

Shamoo, A. E., Albers, R. W. 1973. Na^+-selective ionophoric material derived from electric organ and kidney membranes. *Proc. Nat. Acad. Sci.* **70**:1191

Shamoo, A. E., Myers, M. 1974. Na^+-dependent ionophore as part of the small polypeptide of the $(Na^+ + K^+)$-ATPase from eel electroplax membrane. *J. Membrane Biol.* **19**:163

Shamoo, A. E., Myers, M., Blumenthal, R., Albers, R. W. 1974. Ionophoric material derived from eel membrane preparation. I. Chemical Characteristics. *J. Membrane Biol.* **19**:129

Szabo, G., Eisenman, G., Ciani, S. 1969. The effects of the macrotetralide actin antibiotics on the electrical properties of phospholipid bilayer membranes. *J. Membrane Biol.* **1**:346

Wyman, J. 1948. Heme proteins. *Advanc. Protein Chem.* **4**:407